Article

Self-Construction of Core–Shell and Hollow Zeolite Analcime Icositetrahedra: A Reversed Crystal Growth Process via Oriented Aggregation of Nanocrystallites and Recrystallization from Surface to Core

Chen, Qiao, Xie, Fan, Zhou, and He

J. Am. Chem. Soc., **2007**, 129 (43), 13305-13312• DOI: 10.1021/ja074834u • Publication Date (Web): 04 October 2007

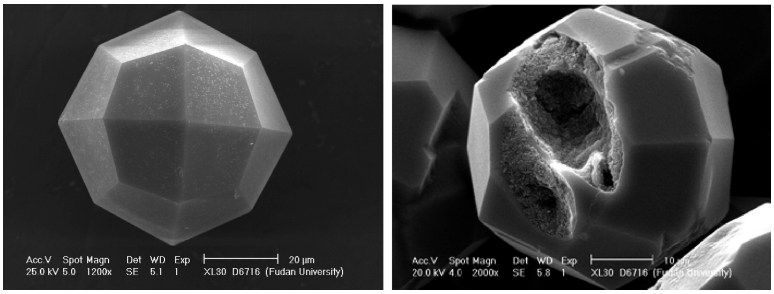

More About This Article

Additional resources and features associated with this article are available within the HTML version:

- Supporting Information
- Links to the 13 articles that cite this article, as of the time of this article download
- Access to high resolution figures
- Links to articles and content related to this article
- Copyright permission to reproduce figures and/or text from this article

View the Full Text HTML

J|A|C|S
ARTICLES
Published on Web 10/04/2007

Self-Construction of Core−Shell and Hollow Zeolite Analcime Icositetrahedra: A Reversed Crystal Growth Process via Oriented Aggregation of Nanocrystallites and Recrystallization from Surface to Core

Xueying Chen,[†] Minghua Qiao,[†] Songhai Xie,[†] Kangnian Fan,[†] Wuzong Zhou,*[,‡] and Heyong He*[,†]

Contribution from the Department of Chemistry and Shanghai Key Laboratory of Molecular Catalysis and Innovative Materials, Fudan University, Shanghai 200433, P. R. China, and School of Chemistry, University of St. Andrews, St. Andrews, Fife KY16 9ST, United Kingdom

Received July 1, 2007; E-mail: wzhou@st-andrews.ac.uk; heyonghe@fudan.edu.cn

Abstract: Zeolite analcime with a core−shell and hollow icositetrahedron architecture was prepared by a one-pot hydrothermal route in the presence of ethylamine and Raney Ni. Detailed investigations on samples at different preparation stages revealed that the growth of the complex single crystalline geometrical structure did not follow the classic crystal growth route, i.e., a crystal with a highly symmetric morphology (such as polyhedra) is normally developed by attachment of atoms or ions to a nucleus. A reversed crystal growth process through oriented aggregation of nanocrystallites and surface recrystallization was observed. The whole process can be described by the following four successive steps. (1) Primary analcime nanoplatelets undergo oriented aggregation to yield discus-shaped particles. (2) These disci further assemble into polycrystalline microspheres. (3) The relatively large platelets grow into nanorods by consuming the smaller ones, and meanwhile, the surface of the microspheres recrystallizes into a thin single crystalline icositetrahedral shell via Ostwald ripening. (4) Recrystallization continues from the surface to the core at the expense of the nanorods, and the thickness of the monocrystalline shell keeps on increasing until all the nanorods are consumed, leading to hollow single crystalline analcime icositetrahedra. The present work adds new useful information for the understanding of the principles of zeolite growth.

Introduction

The past few years have witnessed significant advances in the synthesis of hierarchical nanostructures with controllable size, shape, and well-defined crystalline structure, since they are in high demand for new technological applications.[1−5] As an important category of high-performance materials, zeolites have attracted considerable attention as they are widely used in industry (for instance as catalyst or highly selective adsorbent).[6,7] Recently a huge interest has emerged in the synthesis of zeolite materials with hierarchical structures for better performance in catalysis.[8−12] However, few studies have been carried out to explore the underlying mechanism by which zeolite nanostructures are assembled from primary species under hydrothermal synthetic conditions. An improved understanding of the synthesis mechanism will surely benefit both the design of new zeolites and the fabrication of novel zeolite assemblies such as membranes, monoliths, and functional nanostructures.

Traditional hydrothermal synthetic methods have been playing an important role in the controlled synthesis of zeolite nanostructures.[8−12] There are two basic crystal growth mechanisms in solution systems. One is the so-called Ostwald ripening, and the other is the oriented aggregation process.[13−16]

[†] Fudan University.
[‡] University of St. Andrews.

(1) Antonietti, M.; Göltner, C. *Angew. Chem., Int. Ed. Engl.* **1997**, *36*, 910−928.
(2) Whitesides, G. M.; Grzybowski, B. *Science* **2002**, *295*, 2418−2421.
(3) Cölfen, H.; Mann, S. *Angew. Chem., Int. Ed.* **2003**, *42*, 2350−2365.
(4) Antonietti, M.; Ozin, G. A. *Chem.—Eur. J.* **2004**, *10*, 29−41.
(5) Park, S.; Lim, J. H.; Chung, S. W.; Mirkin, C. A. *Science* **2004**, *303*, 348−351.
(6) Davis, M. E. *Ind. Eng. Chem. Res.* **1991**, *30*, 1675−1683.
(7) Breck, D. W. *Zeolite Molecular Sieves*; John Wiley & Sons: New York, 1974.
(8) (a) Valtchev, V. *Chem. Mater.* **2002**, *14*, 4371−4377. (b) Tosheva, L.; Valtchev, V. *Chem. Mater.* **2005**, *17*, 2494−2513. (c) Valtchev, V.; Mintova, S. *Microporous Mesoporous Mater.* **2001**, *43*, 41−49. (d) Tosheva, L.; Mihailova, B.; Valtchev, V.; Sterte, J. *Microporous Mesoporous Mater.* **2001**, *48*, 31−37. (e) Valtchev, V.; Schoeman, B.; Hedlund, J.; Mintova, S.; Sterte, J. *Zeolites* **1996**, *17*, 408−415.
(9) (a) Holland, B. T.; Abrams, L.; Stein, A. *J. Am. Chem. Soc.* **1999**, *121*, 4308−4309. (b) Huang, L. M.; Wang, Z. B.; Sun, J. Y.; Miao, L.; Li, Q. Z.; Yan, Y. S.; Zhao, D. Y. *J. Am. Chem. Soc.* **2000**, *122*, 3530−3531. (c) Rhodes, K. H.; Davis, S. A.; Caruso, F.; Zhang, B. J.; Mann, S. *Chem. Mater.* **2000**, *12*, 2832−2842.
(10) Lee, Y. J.; Lee, J. S.; Park, Y. S.; Yoon, K. B. *Adv. Mater.* **2001**, *13*, 1259−1263.
(11) (a) Dong, A. G.; Wang, Y. J.; Tang, Y.; Ren, N.; Zhang, Y. H.; Yue, Y. H.; Gao, Z. *Adv. Mater.* **2002**, *14*, 926−929. (b) Wang, Y. J.; Tang, Y.; Dong, A. G.; Wang, X. D.; Ren, N.; Shan, W.; Gao, Z. *Adv. Mater.* **2002**, *14*, 994−997.
(12) (a) Jacobsen, C. J. H.; Madsen, C.; Houzvicka, J.; Schmidt, I.; Carlsson, A. *J. Am. Chem. Soc.* **2000**, *122*, 7116−7117. (b) Tao, Y. S.; Kanoh, H.; Kaneko, K. *J. Am. Chem. Soc.* **2003**, *125*, 6044−6045. (c) Schmidt, I.; Boisen, A.; Gustavsson, E.; Ståhl, K.; Pehrson, S.; Dahl, S.; Carlsson, A.; Jacobsen, C. J. H. *Chem. Mater.* **2001**, *13*, 4416−4418. (d) Cho, S. I.; Choi, S. D.; Kim, J. H.; Kim, G. J. *Adv. Funct. Mater.* **2004**, *14*, 49−54. (e) Kim, S. S.; Shah, J.; Pinnavaia, T. J. *Chem. Mater.* **2003**, *15*, 1664−1668.

In the former, it is assumed that the growth of crystals occurs via atom-by-atom addition to existing nuclei and the morphology of a polyhedron is normally the end result.[13,14] According to the well-established geometrical theory of crystal growth, the so-called Bravais−Friedel−Donnay−Harker (BFDH) law[17−19] and Hartman−Perdok approach,[20] the as-grown crystal morphology is dominated by the slow-growing faces because the fast-growing faces may grow out and not be represented in the final crystal habit. However, in an oriented aggregation process, primary meso-, micro-, or nanostructured building blocks are organized to share an identical crystallographic orientation and join at the plane interfaces to form single-crystalline architectures.[15,16]

During the course of our studies of the crystal growth of Co nanoparticles, we found that the detailed process of crystal growth might be much more complicated than what we had known. Co nanoparticles on the Mg_2SiO_4 surface self-assembled into large aggregates and eventually recrystallized into single crystalline polyhedra.[21] However, we did not observe any direct evidence to show the detailed process of the recrystallization since the transformation was too fast to be monitored. Thus, it was difficult to conclude whether the recrystallization took place from the surface of the aggregates to the core or in the reverse direction. Herein, we report the preparation of zeolite analcime with a hierarchical core−shell and hollow icositetrahedron architecture. By systematically investigating the growth process, for the first time we demonstrated that the complex geometrical structure can be built via the route of "Nanocrystallites" − "oriented Aggregation" − "surface Recrystallization" − "Single crystals", designated the NARS route in its short form. Perfect icositetrahedra were developed on the surface of polycrystalline microspheres, and the crystal growth extended from the surface to the core. The discovery of this novel phenomenon with a reversed direction of crystal growth may have an important implication in the fields of nanoscience, materials science, and mineralogy. The main reason to choose zeolite analcime here as the target material is that its crystal growth takes several days to complete and can be monitored easily by collecting samples at different growth stages for studies of their microstructures. Moreover, analcime is one of the very few zeolites which appear with regular icositetrahedral morphology.[22] Thus, it is very convenient for us to observe the morphology transformation of analcime at different crystal growth stages and record the detailed process of recrystallization.

Experimental Section

Raney Ni−Al alloy was added into an aqueous sodium silicate solution in batches under vigorous stirring at 90 °C. The mixture was continuously stirred for 2 h for further dissolution of Al. Ethylamine was then added, followed by the addition of sulfuric acid. The mixture with a nominal molar composition of 1 SiO_2/1 Na_2O/0.22 Ni/0.48 Al/1.26 $C_2H_5NH_2$/0.63 H_2SO_4/19 H_2O was transferred into a Teflon-lined stainless steel autoclave for crystallization at 180 °C from 6 h to 22 days. The products were washed with distilled water six times, separated from the residual Raney Ni by magnetic attraction, washed with ethanol six times, dried at ambient temperature, and finally calcined at 550 °C in air for 6 h.

The bulk composition of the analcime sample was determined by inductively coupled plasma-atomic emission spectroscopy (ICP-AES, Thermo Elemental IRIS Intrepid). The Brunauer−Emmett−Teller (BET) surface area and the pore volume were measured by N_2 adsorption/desorption isotherms at −196 °C on a Micromeritics TriStar 3000 adsorption apparatus. The powder X-ray diffraction (XRD) patterns were collected on the Bruker AXS D8 Advance X-ray diffractometer using Cu Kα radiation. The morphology and microstructure were examined by using scanning electron microscopy (SEM) on a Philips XL30 electron microscope operating at 20 to 30 kV. To improve electrical conductivity, the specimens were coated with a thin layer of Au. Chemical compositions of individual particles were detected by using an energy dispersive X-ray emission analyzer (EDX). Transmission electron microscopy (TEM) observations were conducted on a JEOL JEM-2011 electron microscope operating at 200 kV, to which an EDX system was also attached. Single-crystal XRD experiments were performed on a Bruker AXS SMART X-ray diffractometer equipped with a CCD area detector and a normal-focus, 2.4 kW sealed-tube X-ray source (Mo Kα radiation, $\lambda = 0.710\ 73$ Å) operating at 50 kV and 30 mA. About 1.3-hemispheres of intensity data were collected with a scan width of 0.30° in ω and an exposure time of 30 s per frame.

Results and Discussion

Structure of the Zeolite Analcime Icositetrahedra. The specimens were initially characterized by SEM. The zeolite analcime product after reaction for 8 days showed uniform particle size (∼50 μm in diameter) and high yield (Figure 1a). All the particles can be characterized as icositetrahedra(211) with 24 identical {211} faces of a cubic structure, which possesses four 3-fold axes and three 4-fold axes, and belongs to the cubic $m3m$ point group.[19] Another type of common icositetrahedron, icositetrahedron(311) where the 24 faces are {311},[23] and other types of polyhedra were not observed. As shown in Figure 1b, most crystals are clearly facetted, although some joined icositetrahedra can also be occasionally observed. EDX of the specimen (Figure 1c), supported by the ICP analysis, gave an atomic ratio of 1.0 Na/2.4 Si/1.0 Al within the range of the Si/Al ratio of zeolite analcime.[7,24] All the observed peaks in the powder XRD pattern (Figure 2) can be indexed onto the cubic unit cell of analcime with the unit cell parameter $a =$ 1.360 nm (PDF card No. 41-1478). Both EDX and XRD confirmed that the product was pure cubic analcime without detectable nickel species or other impurities.

What is special for the analcime icositetrahedra prepared in the present work is that the perfect icositetrahedral morphology shown in Figure 1 was not developed from the attachment of ions to nuclei in the centers of the crystals as predicted by the classical crystal growth theory. When the icositetrahedral particles were crushed, SEM images reveal a unique core−shell structure, i.e., a core with randomly stacked nanorods (Figure 3a and 3b) and a single crystalline icositetrahedral shell. The

(13) Ostwald, W. *Lehrbruck der Allgemeinen Chemie*; Leipzig, Germany, 1896; Vol. 2, Part 1.
(14) Boistelle, R.; Astier, J. P. *J. Cryst. Growth* **1988**, *90*, 14−30.
(15) Banfield, J. F.; Welch, S. A.; Zhang, H. Z.; Ebert, T. T.; Penn, R. L. *Science* **2000**, *289*, 751−754.
(16) Penn, R. L.; Banfield, J. F. *Science* **1998**, *281*, 969−971.
(17) Bravais, A. *études Cristallographic*; Gauthier-Villars: Paris, 1866.
(18) Friedel, M. G. *Bull. Soc. Fr. Mineral. Cristallogr*. **1907**, *30*, 326−455.
(19) Donnay, J. D. H.; Harker, D. *Am. Mineral*. **1937**, *22*, 446−467.
(20) Hartman, P.; Perdok, W. G. *Acta Crystallogr*. **1955**, *8*, 49−52, 521−524, 525−529.
(21) (a) Xie, S. H.; Zhou, W. Z.; Zhu, Y. Q. *J. Phys. Chem. B* **2004**, *108*, 11561−11566. (b) Zhu, Y. Q.; Hsu, W. K.; Zhou, W. Z.; Terrones, M.; Kroto, H. W.; Walton, D. R. M. *Chem. Phys. Lett.* **2001**, *347*, 337−343.
(22) Agger, J. R.; Shöâeè, M.; Mistry, M.; Slater, B. *J. Cryst. Growth* **2006**, *294*, 78−82.
(23) Saito, Y.; Yatsuya, S.; Mihama, K.; Uyeda, R. *Jpn. J. Appl. Phys.* **1978**, *17*, 291−297.
(24) Ghobarkar, H.; Franke, W. *Cryst. Res. Technol*. **1986**, *21*, 1071−1075.

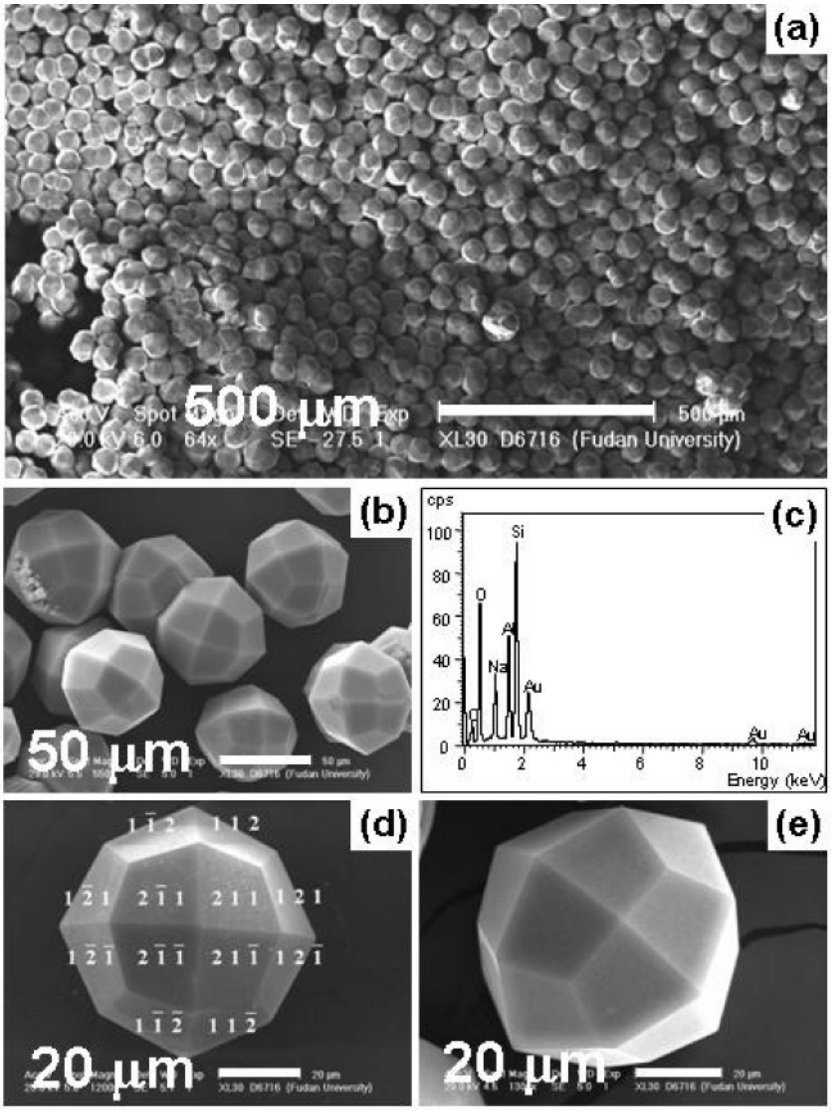

Figure 1. SEM images of zeolite analcime with crystal growth time of 8 days. (a, b) Low magnification images showing a high yield and uniform particle size of the specimen. (c) EDX spectrum. (d, e) Enlarged images showing perfect icositetrahedra (211).

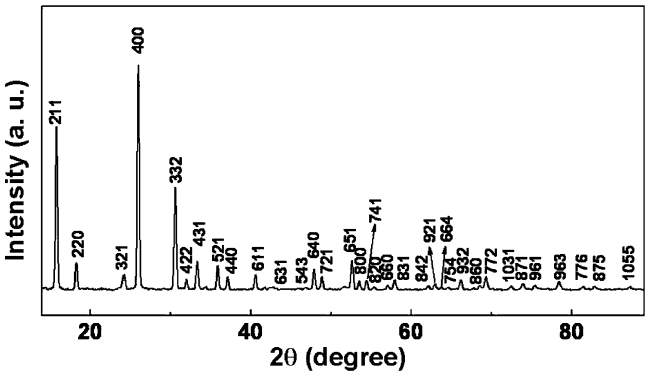

Figure 2. Powder XRD pattern of zeolite analcime prepared with crystal growth time of 8 days, indexed to the cubic unit cell with $a = 1.360$ nm.

dimensions of these nanorods are mainly from 50 to 150 nm in width and 60 nm to 2 μm in length (Figure 3b−3e). All the icositetrahedra have this unusual structure, suggesting an alternative crystal growth route.

Figures 3b and 3c further show that the interior nanorods have well developed hexagonal cross section. All the nanorods are single crystalline and have the same structure and composition of analcime, as determined by selected area electron diffraction (SAED), high-resolution TEM (HRTEM), and EDX (Figure 3e and 3f). It is noted that most SAED patterns from the nanorods are along the ⟨211⟩ zone axes without specimen tilting (Figure 3e). The reason for this is that the nanorods have six {211} side facets with the long axis parallel to the [111] direction and have a preferential orientation to the supporting film.[25] The appearance of the $(1\bar{1}0)$ diffraction spot is attributed to multiple scattering, which should be systematically absent for the $Ia\bar{3}d$ space group of analcime.

Figure 4 shows that the analcime icositetrahedra exhibit type IV N_2 physisorption isotherms with a hysteresis loop above $P/P_0 = 0.4$, signifying the presence of mesopores.[26] The mesoporosity was further verified by the corresponding pore size distribution curve (see inset in Figure 4) calculated from the adsorption branch using the Barrett−Joyner−Halenda (BJH) algorithm. These mesopores can be reasonably ascribed to voids among the nanorods, further proving the polycrystalline core structure in the specimen.

(25) Wang, Z. L. *J. Phys. Chem. B* **2000**, *104*, 1153−1175.
(26) Gregg, S. J.; Sing, K. S. W. *Adsorption, Surface Area and Porosity*, 2nd ed.; Academic Press: London, 1982.

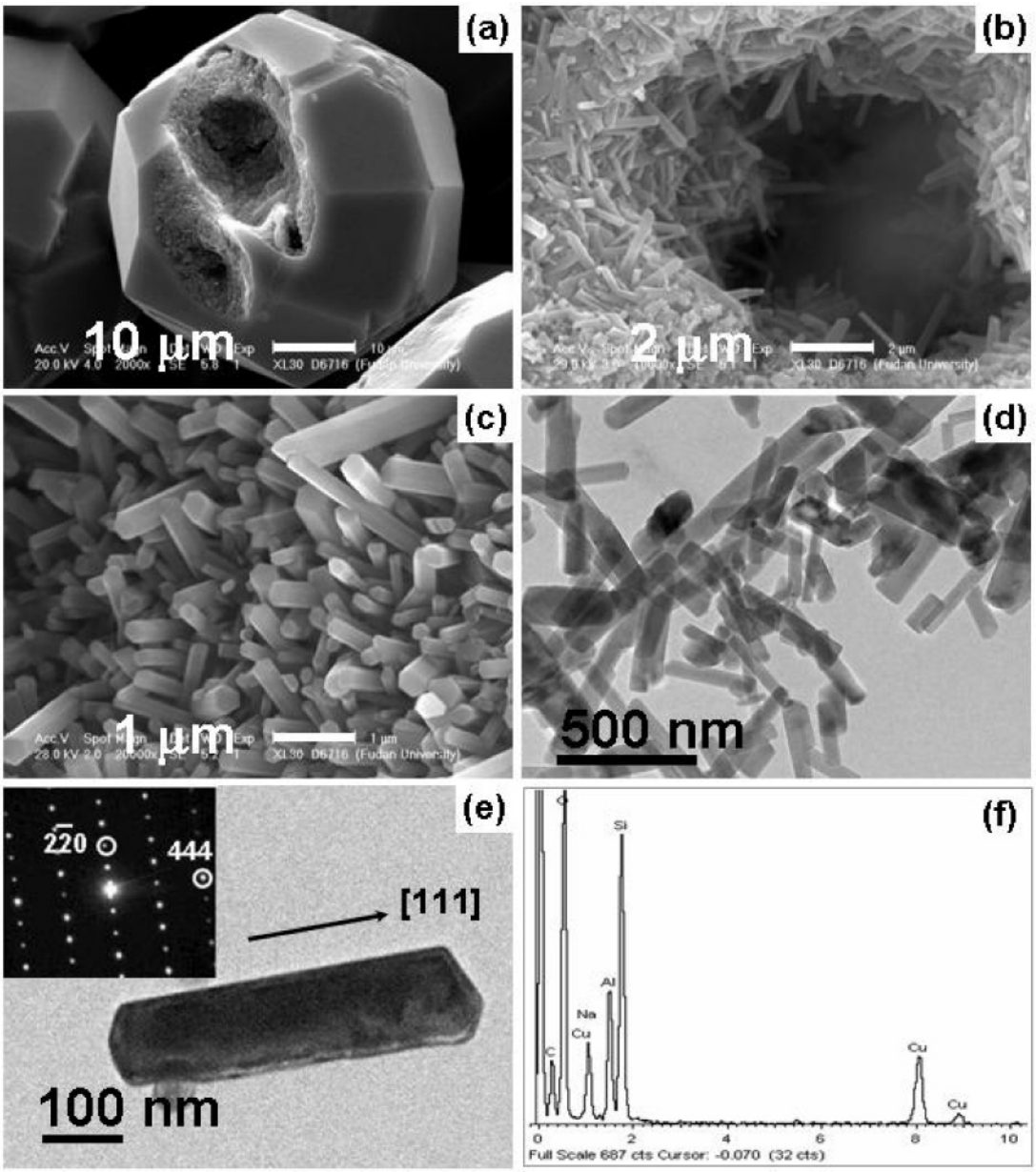

Figure 3. SEM images of zeolite analcime with crystal growth time of 8 days. (a) An intentionally broken icositetrahedron showing a polycrystalline core. (b) The hole on the damaged icositetrahedron showing nanorods of analcime inside. (c) Enlarged SEM image of the nanorods showing hexagonal cross sections. (d) Low magnification TEM image of the nanorods in the icositetrahedron. (e) TEM image of an individual nanorod and the corresponding SAED pattern indexed onto the cubic analcime structure viewed from the [11$\bar{2}$] zone axis. (f) Typical EDX spectrum of the nanorods.

Single-crystal XRD further verified the structure of the icositetrahedra, which consists of a polycrystalline core and a single crystalline shell. The diffraction patterns from all selected particles show an overlap of polycrystalline diffraction rings and single crystalline patterns with sharp diffraction spots. A typical single-crystal XRD pattern is shown in Figure 5a.

Zeolite Analcime at Intermediate Stages of Hydrothermal Synthesis. To unveil the formation mechanism of the core−shell icositetrahedra, specimens were collected after crystal growth times of 6, 16, 20, 24, and 72 h. The powder XRD patterns in Figure 6 show that hydrothermal synthesis for 6 h did not lead to any detectable crystalline phase. However, the cubic analcime phase had already emerged after 16 h of the reaction. With increasing the preparation time, the diffraction peaks were intensified gradually.

SEM and TEM images of the specimens collected at different growth stages are presented in Figure 7. At the early stage of 16 h, Figure 7a and 7b show that discus-shaped aggregates formed with a typical diameter of about 2 μm and a thickness of about 400 nm, which are constituted by nanoplatelets about 20 nm in diameter with a polygonal morphology (inset in Figure 7b, bottom right). SAED and HRTEM examinations of the nanoplatelets verified that they were monocrystalline.

What is extraordinary for the disci is that all the nanoplatelets constituting the disci are preferentially oriented along the [111] direction, as evidenced by the SAED pattern which looks like a single crystalline diffraction pattern (inset in Figure 7b, upper left). HRTEM results unambiguously verified the perfectly oriented structure of the disci. Figure 7c shows the HRTEM image taken from the marked elliptical area of a discus in Figure 7b. It is clearly seen that the two nanoplatelets within the discus

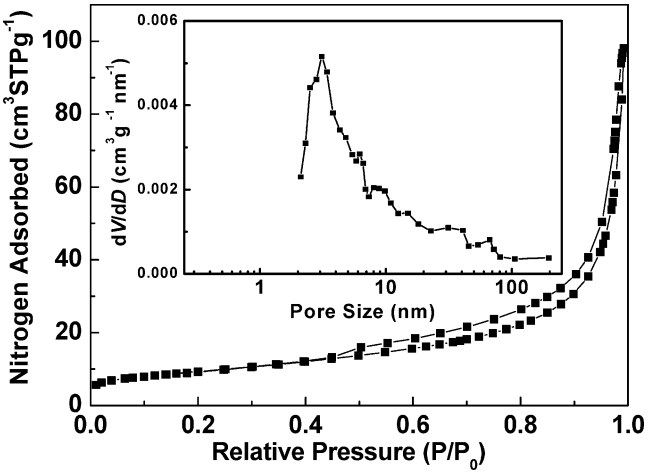

Figure 4. Nitrogen adsorption−desorption isotherms of the analcime icositetrahedra with crystal growth time of 8 days. The inset is the pore size distribution curve calculated from the adsorption branch using the Barrett−Joyner−Halenda (BJH) algorithm.

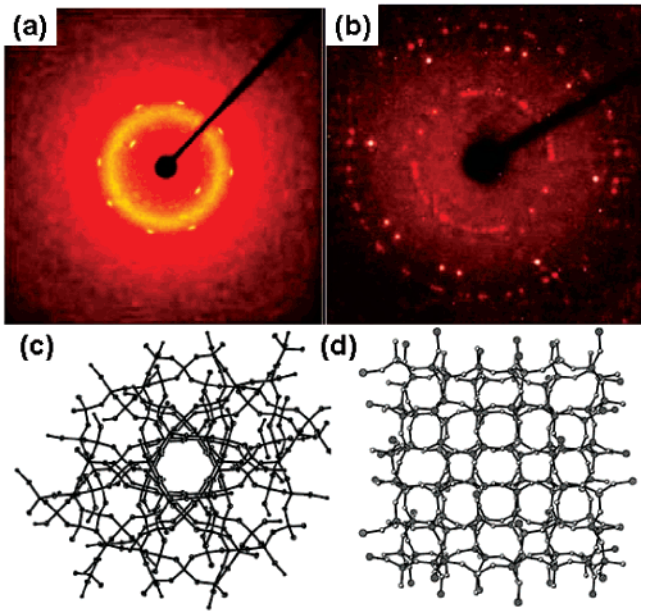

Figure 5. (a) Single-crystal X-ray diffraction pattern from an analcime icositetrahedron with crystal growth time of 8 days, showing both single crystalline pattern and polycrystalline pattern. (b) Single-crystal X-ray diffraction pattern of a typical icositetrahedron of analcime with crystal growth time of 22 days, showing typical single crystalline pattern. The structure was solved by direct methods followed by successive difference Fourier methods. The solved framework structure of analcime icositetrahedron based on the diffraction pattern in (b), showing projection down the [111] threefold rotation axis (c) and irregular channels formed by highly distorted eight-membered rings (d).

intimately contact each other. The parallelism and overlap of the lattice fringes of the nanoplatelets demonstrate that crystallographic axes of the primary nanoplatelets are parallel, providing direct evidence for the oriented aggregation growth mechanism of the sample.[27,28] Figure 7f shows the profile view of a discus, revealing its thickness and again the single crystalline-like structure. Although oriented aggregation has been identified in other nanomaterials,[27,28] such a perfect alignment of zeolite

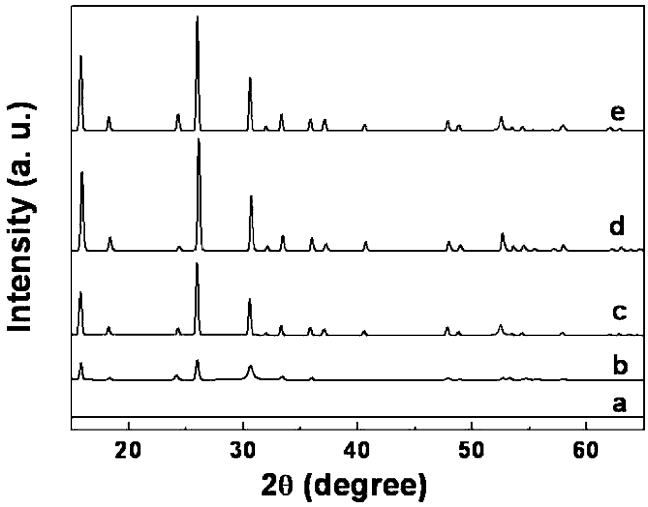

Figure 6. Powder XRD patterns of the analcime specimens prepared at different hydrothermal synthesis stages for (a) 6, (b) 16, (c) 20, (d) 24, and (e) 72 h. All the XRD patterns are identical to those in Figure 2.

nanocrystallites has not been reported and can be regarded as a good example of the phenomenon.

When the hydrothermal process was prolonged to 20 h, most disci further aggregate into regular microspheres with a typical diameter of about 30 μm (Figure 7g). Microspheres that were not well developed were also present, as exemplified in Figure 7d. In Figure 7d and 7e, it is clearly seen that the microspheres contain self-assembled disci. A close examination of the regular microspheres (Figure 7h) revealed that the surface is rough without any facets. Some nanocrystallites can even be identified on the sphere surface. However, some areas of the surface have recrystallized into large and smooth inlaid domains. TEM observations (Figure 7i) demonstrate that the average particle size of the nanoplatelets constituting the disci has become larger and the shape has changed from polygonal to near rodlike with slight elongation along the [111] direction.

After the hydrothermal synthesis for 24 h, the {211} facets were developed for all the microspheres as shown in Figure 7j, when the average size of the microspheres increased to about 50 μm in diameter and the nanocrystallites constituting the microspheres gradually grew into larger nanorods with increasing [111] elongation (Figure 7l). It is interesting to see that at this stage the facets are still rough and the microspheres are not yet completely covered by the recrystallized shell. There are some rodlike nanocrystals embedded in the aperture of the {211} faces as exemplified in Figure 7k, indicating that the icositetrahedra are actually built from nanorods.

When the synthesis time was further increased to 72 h, the {211} crystal habits became much more apparent. After successive reaction for 8 days, perfect icositetrahedral morphology was observed for most particles, as has been shown in Figure 1. During this period, the increase in the particle size was not significant. Even after a hydrothermal synthesis of 22 days, the particle size remained 50−60 μm (Figure 8c). On the other hand, ripened nanorods with a well developed hexagonal cross section grew underneath the single crystalline icositetrahedral shell (Figure 3). This can be explained by the Ostwald ripening process, first established one century ago by Wilhelm Ostwald:[13,14] when two particles with different sizes attached

(27) Zhang, D. F.; Sun, L. D.; Yin, J. L.; Yan, C. H.; Wang, R. M. *J. Phys. Chem. B* **2005**, *109*, 8786−8790.
(28) Pacholski, C.; Kornowski, A.; Weller, H. *Angew. Chem., Int. Ed.* **2002**, *41*, 1188−1191.

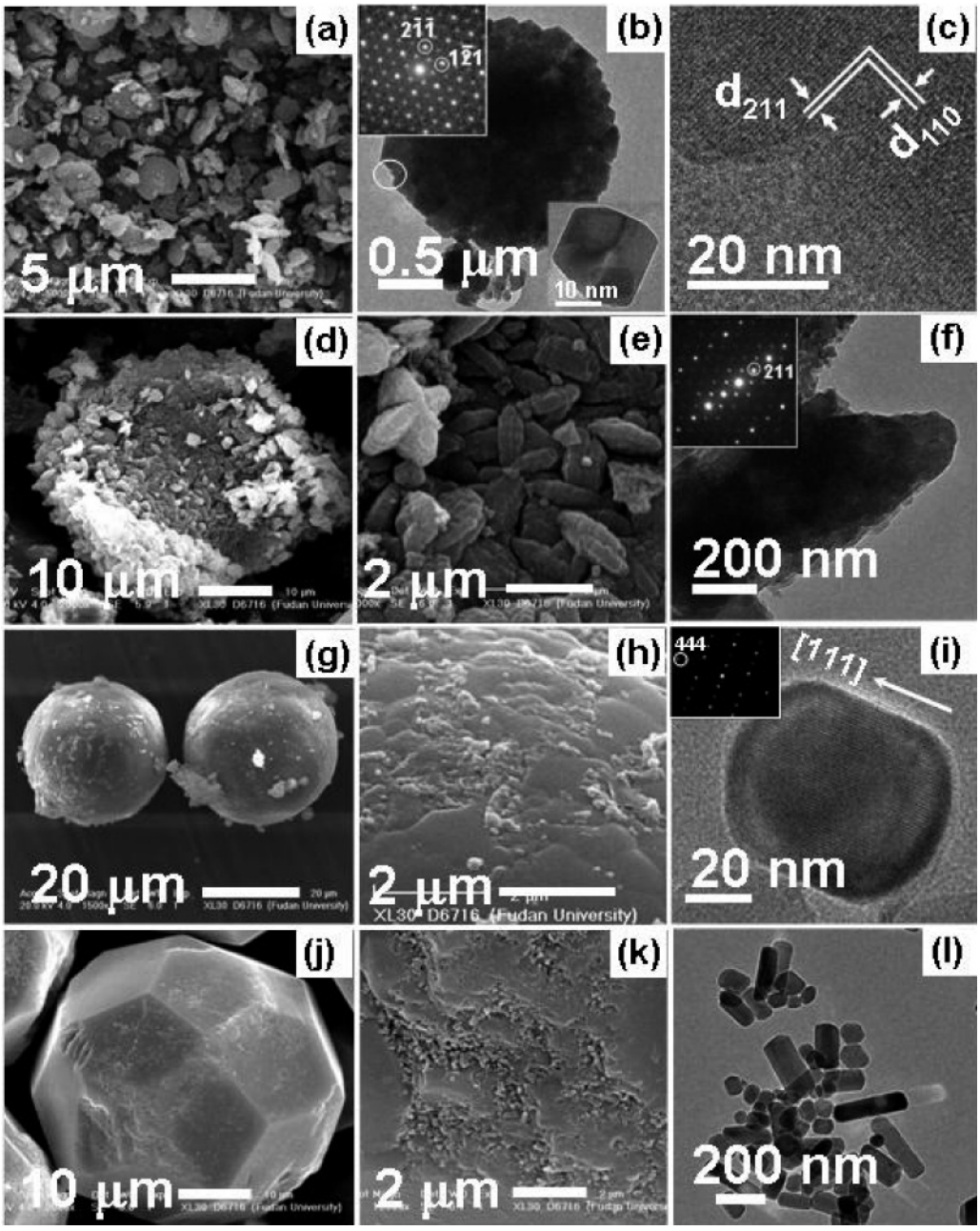

Figure 7. (a) SEM image of separated discus-shaped aggregates after growth for 16 h. (b) TEM image of a single discus on the projection along the short axis of the discus, showing the aggregation of nanoplatelets. The insets are the corresponding SAED pattern from the whole discus (upper left) and the TEM image of a single nanoplatelet (bottom right). The viewing direction for the SAED pattern is along the [111] zone axis of the zeolite structure. The appearance of the weak {110} dots is due to multiple scattering. (c) HRTEM image of the connecting area marked by an ellipse in (b), demonstrating that the lattice planes of the nanoplatelets are perfectly aligned. (d) SEM image of a spherical cluster after crystal growth for 20 h. (e) Enlarged SEM image of the spherical cluster in (d) showing that the aggregate is assembled by disci. (f) A profile view of a single discus and the corresponding SAED pattern (inset). (g) SEM image of regular microspheres from the specimen after 20 h hydrothermal synthesis. (h) Enlarged SEM image of a microsphere in (g) showing partial recrystallization without any facets. (i) Typical TEM image and the corresponding SAED pattern (inset) of a rodlike nanocrystal constituting the microspheres obtained by crushing the microspheres. (j) SEM image of the specimen after 24 h hydrothermal synthesis, showing partial formation of the {211} facets of icositetrahedron. (k) Enlarged SEM image of the icositetrahedron in (j) showing that many rodlike nanocrystals are embedded in the aperture of the faces. (l) TEM image of nanorods underneath the recrystallized shell.

to each other, energetic factors will drive the large particle to grow, drawing from the small one, which shrinks. In a cluster of nanoparticles, fewer and larger crystals may form that have smaller surface-to-volume ratios compared to the smaller particles, thus reducing the energy of the entire system. The reason for the preferential growth along the [111] direction forming the nanorods is that these nanorods were developed from the above-mentioned nanoplatelets in the disci where they all oriented along the [111] direction (Figure 7b and 7c). This type of aggregation may suppress the crystal growth along other directions.

What was happening during the hydrothermal synthesis from 3 days to 22 days, when both the particle size and the icositetrahedral morphology were virtually unchanged, is even more fascinating. SEM images (Figure 8a and 8b) revealed that the thickness of the shell increased from about 200 nm (3 days)

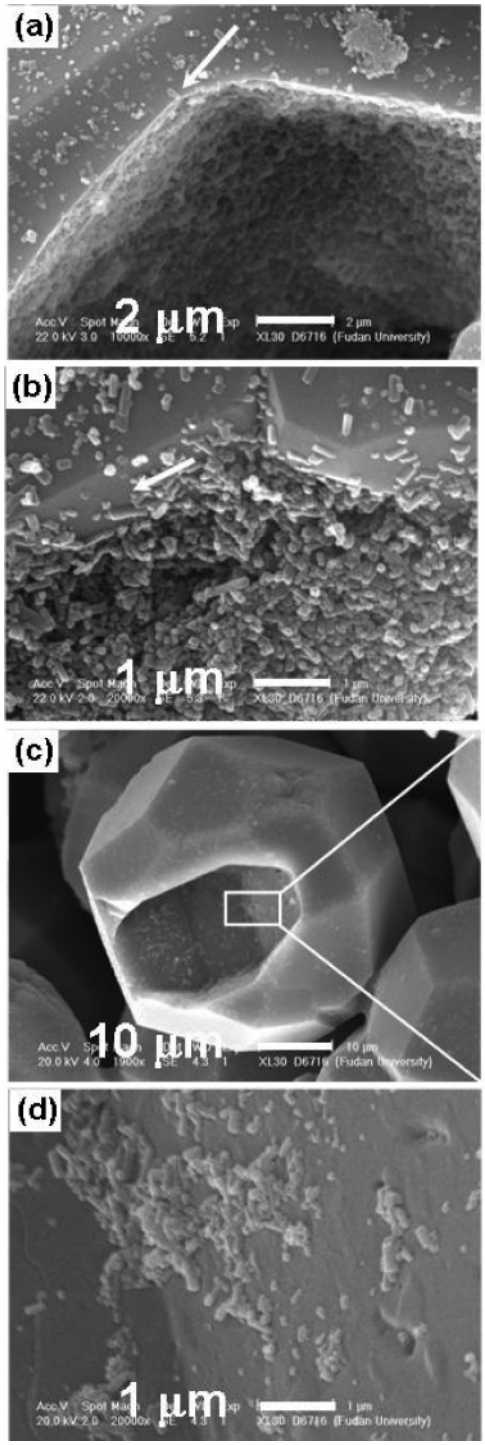

Figure 8. SEM images of crushed icositetrahedra after hydrothermal synthesis for (a) 3, (b) 8, and (c) 22 days. (d) Enlarged SEM image of the interior structure of the icositetrahedron in (c) as marked by the rectangle. The arrows indicate the cross sections of the single crystalline shells, showing the thicknesses of the shells.

to about 600 nm (8 days). The single crystalline shell had been *eating* the nanorods on its inner surface, and after 22 days, almost all the nanorods were consumed (Figure 8c and 8d). The whole icositetrahedral particles became nearly single crystalline, although a hole more likely existed in each particle (Figure 8c) after the transformation from nanorods to single crystals. From these hollow analcime icositetrahedra, single crystalline diffraction patterns can be obtained (Figure 5b) and it has been revealed that the topological framework structure is identical to the cubic phase with a space group of $Ia\bar{3}d$.[29] This type of recrystallization can be regarded as a novel Ostwald ripening process.

Formation Mechanism of Zeolite Analcime Icositetrahedra. Combined with the investigations shown above, the formation process of the core−shell and hollow analcime icositetrahedra architecture can be depicted as follows, which is also schematically illustrated in Figure 9.

(1) Primary analcime nanoplatelets (∼20 nm) which expose {111} faces are formed initially under the synthetic condition. It is understandable that cubic analcime usually does not expose {111} faces which possess high surface energy.[19,24] However, the crystal morphology depends not only on intrinsic crystal structure but also on the synthesis conditions.[19,30] In addition to the above-mentioned oriented aggregation, leading to suppression of the crystal growth along all directions other than [111], the fact that {111} faces prevail in the present case may also be due to the special synthesis conditions, particularly the presence of ethylamine which possibly acts as an organic ligand interacting with the {111} planes of analcime and leads to the inhibition of crystal growth in the [111] direction at an early stage of the formation of the nanoplatelets and reduces the potential of possible aggregation on the (111) surface.

(2) The [111]-oriented nanoplatelets stack spontaneously to form vectorially aligned discus-shaped aggregates via an oriented aggregation mechanism. The process is somewhat analogous to the 3D assembly route previously described for CuO[31] and SnO_2.[32]

(3) The discus-shaped aggregates further self-assemble into polycrystalline microspheres. The increase in the size of the microspheres slows down significantly when the size approaches about 50 μm in diameter.

(4) The nanoplatelets composing the microspheres undergo conventional Ostwald ripening and continuously grow into large nanorods. Meanwhile, the surface of the microspheres recrystallizes into a single crystalline thin shell, and the icositetrahedral morphology is gradually developed. Thus, unique icositetrahedra with a polycrystalline core and a single crystalline shell are formed.

(5) The single crystalline icositetrahedral shell increases in thickness by *eating* at the nanorods on the inner surface via Ostwald ripening until all the nanorods are consumed, and finally single-crystal icositetrahedra with a small hole are generated.

It should be noted that, among the well-established classic crystal growth theories, the Bravais law relates the crystal facets to the growth rate of the faces based on the assumption that crystal is developed from a single nucleus and extends outward. Curie and Wulff paid more attention to the surface of a crystal rather than its interior structure. It was believed that the equilibrium shape of a free crystal is the shape that minimizes its surface free energy.[33,34] In the case of analcime, it has been well investigated that the {211} facets have the lowest energy[19] and so does the icositetrahedra consisting of 24 {211} facets. Therefore, the crystal growth of analcime presented here can

(29) Taylor, W. H. *Z. Kristallogr.* **1930**, *74*, 1−19.
(30) Gehrke, N.; Cölfen, H.; Pinna, N.; Antonietti, M.; Nassif, N. *Cryst. Growth Des.* **2005**, *5*, 1317−1319.
(31) Liu, B.; Zeng, H. C. *J. Am. Chem. Soc.* **2004**, *126*, 8124−8125.
(32) Yang, H. G.; Zeng, H. C. *Angew. Chem., Int. Ed.* **2004**, *43*, 5930−5933.
(33) Curie, P. *Bull. Soc. Fr. Mineral. Cristallogr.* **1885**, *8*, 145−150.
(34) Wulff, G. *Z. Kristallogr.* **1901**, *34*, 449−480.

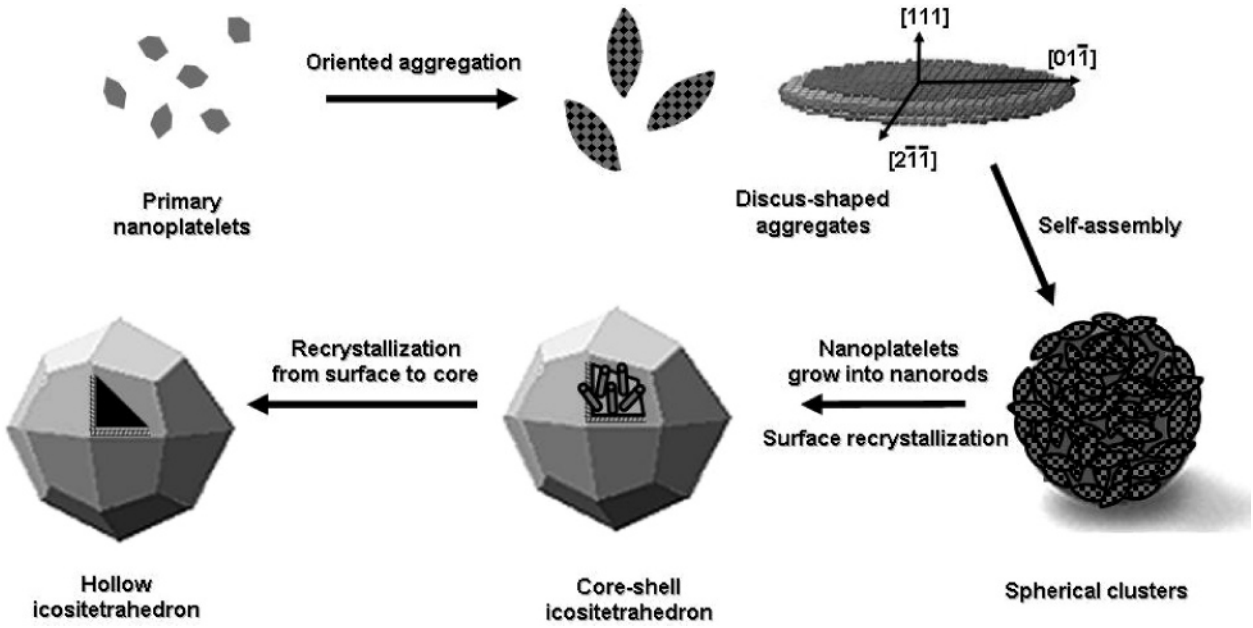

Figure 9. Proposed growth process of the core−shell and hollow analcime icositetrahedra.

be a good example of the Curie−Wulff law. However, how the different surface areas communicated with each other during the very early stage of recrystallization to form an icositetrahedral single crystalline thin shell in a concerted fashion is still unknown. Nevertheless, the present results revealed a new phenomenon of crystal growth, which may occur in growth processes of many other crystals but has been neglected in the past when crystal growth at early stages was not sufficiently investigated.

Conclusion

We have established a novel and facile method for the fabrication of zeolite analcime with hierarchical core−shell or hollow icositetrahedron architecture. By careful analysis of the products at different growth stages, it is demonstrated that the formation of the single crystalline polyhedra does not start from a nucleus and extend outward. It actually follows a reversed route based on oriented aggregation of nanocrystallites, the NARS route; i.e., recrystallization starts at the surface of the polycrystalline microspheres and extends inward. When the crystallites grow up to a nanoscale size, there are two possible ways for crystal growth. One is the further growth of individual nanocrystallites. The other is the aggregation of the nanocrystallites. In the latter, the crystal growth of individual nanocrystallites is greatly suppressed. When the aggregation dominates the process, the reverse route of crystal growth may be adopted. Consequently, the new formation mechanism may not be unique to analcime. Investigations of crystal growth of other zeolite materials are currently carried out in these laboratories in order to find out more material systems in which crystal growth follows the NARS route.

Acknowledgment. This work was supported by the National Basic Research Program of China (2006CB202502, 2003CB615807), the Fok Yin Tong Education Foundation (104022), the NSFC (20673025, 20421303 and 20633030), and the Shanghai Science and Technology Committee (06JC14009, 06DJ14006). W.Z.Z. thanks Fudan University for the Senior Visiting Scholarship and Prof. David J. Cole-Hamilton and Dr. Joe A. Crayston for useful discussions.

JA074834U